Supplementary Material for: The Anharmonic Origin of the Giant Thermal Expansion of NaBr

Y. Shen,[1,*] C. N. Saunders,[1] C. M. Bernal,[1] D. L. Abernathy,[2] M. E. Manley,[3] and B. Fultz[1,†]

[1] *Department of Applied Physics and Materials Science, California Institute of Technology, Pasadena, California 91125, USA*
[2] *Neutron Scattering Division, Oak Ridge National Laboratory, Oak Ridge, Tennessee 37831, USA*
[3] *Material Science and Technology Division, Oak Ridge National Laboratory, Oak Ridge, Tennessee 37831, USA*

(Dated: June 9, 2020)

I. COMPARING THE THERMAL EXPANSION IN QUASIHARMONIC AND ANHARMONIC THEORIES

A. Classical Thermodynamics

The (volumetric) thermal expansion coefficient, β, is defined as

$$\beta = \frac{1}{V}\frac{\mathrm{d}V}{\mathrm{d}T} \tag{1}$$

at $P = 0$, or at a constant pressure. This Section I obtains β from the thermodynamic free energy $F(V,T)$, which includes the variables of Eq. 1. Classical thermodynamics provides relationships involving partial derivatives of F with respect to V and T. Thermal expansion requires both types of partial derivatives to second order. Expansion is a change in volume, of course, but thermal expansion occurs with a change of temperature.

We start with a thermodynamic identity

$$\beta = -\frac{1}{B_T}\frac{\partial^2 F}{\partial T \partial V}\ , \tag{2}$$

where B_T is the isothermal bulk modulus, defined as

$$B_T = -V\frac{\partial P}{\partial V} = V\frac{\partial^2 F}{\partial V^2}\ . \tag{3}$$

Thus, we have

$$\beta = -\frac{1}{V}\left(\frac{\partial^2 F}{\partial T \partial V}\right) \Big/ \left(\frac{\partial^2 F}{\partial V^2}\right)\ . \tag{4}$$

One strategy to calculate thermal expansion is to solve for $f(T,V) \triangleq \dfrac{\partial F}{\partial V} = 0$ for $V = V(T)$ in quasiharmonic or anharmonic models, and then obtain the thermal expansion coefficient from Eq. 1. This is done for the quasiharmonic approximation in Sect. III with Fig. 4. Here we employ an alternative strategy of calculating Eq. 4 directly. The two approaches are equivalent because

$$\frac{\mathrm{d}V}{\mathrm{d}T} = -\left(\frac{\partial f}{\partial T}\right) \Big/ \left(\frac{\partial f}{\partial V}\right) = -\left(\frac{\partial^2 F}{\partial T \partial V}\right) \Big/ \left(\frac{\partial^2 F}{\partial V^2}\right)\ . \tag{5}$$

B. Phonon Statistical Mechanics

We address the underlying physics by calculating the phonon free energy, ignoring possible contributions from electronic or magnetic excitations. The key quantities are the energies $\{\hbar\omega_i\}$, where ω_i is the frequency of a phonon

* yshen@caltech.edu
† btf@caltech.edu

added to the ith vibrational mode. In general, this frequency depends on V and T, $\omega_i(V,T)$. In the "quasiharmonic approximation" (QHA), the ω_i and the phonon free energy depend only on V. In the QHA, the effects of T are only from the occupancies of phonon modes. The QHA is convenient for calculating thermal expansion, requiring only a set of mode Grüneisen parameters.

It was recently proved that the QHA gives the leading term of the quantity $\partial F/\partial V$ [1], also [2]. This does not guarantee that the QHA gives the leading term of the thermal expansion coefficient, however, because a temperature derivative is still needed. (For example, consider the functional $y = y_0 + \Delta y$, where $y_0 = 100 + 0.001 \sin x$ and $\Delta y = \sin x$. Here the x-derivative is dominated by the small term Δy, rather than the leading term y_0.)

Less well known are anharmonic theories of thermal expansion developed with many-body theory [3, 4]. To our knowledge, there has been no direct comparison of thermal expansion from the QHA and anharmonic theory, so the goal of this section is an comparison of their relative importance.

Ignoring the entropy from free electrons or magnetic excitations, for a simple solid with N atoms the Helmholtz free energy originates with the electronic energy, i.e., the internal energy of the lattice, U_0, plus the free energy from phonons

$$\begin{aligned} F &= U_0 + F_{\rm ph} \ , \\ F &= U_0 + \left\langle \sum_{\mathbf{k},j} \left[\frac{1}{2}\hbar\omega_{\mathbf{k},j} + k_{\rm B}T \ln\left(1 - e^{-\frac{\hbar\omega_{\mathbf{k},j}}{k_{\rm B}T}}\right)\right]\right\rangle_{\rm BZ} \ . \end{aligned} \tag{6}$$

where $\hbar\omega_{\mathbf{k},j}$ is the phonon energy at the $\mathbf{k}$-point for the jth phonon branch. The sum is taken over all phonon branches and $\mathbf{k}$-points in reciprocal space, and $\langle ... \rangle_{\rm BZ}$ is the average over the first Brillouin zone. For clarity in what follows, the subscripts of ω are suppressed.

Because the free energy depends on V and T, we expect $U_0 = U_0(V,T)$ and $\omega = \omega(V,T)$. Derivatives of these quantities are needed for Eq. 4. The volume derivative is essential for expansion

$$\begin{aligned} \frac{\partial F}{\partial V} &= \frac{\partial U_0}{\partial V} + \left\langle \sum \frac{\hbar}{2}\frac{\partial \omega}{\partial V} + \frac{k_{\rm B}T}{1 - e^{-\frac{\hbar\omega}{k_{\rm B}T}}}\left(-e^{-\frac{\hbar\omega}{k_{\rm B}T}}\right)\left(-\frac{\hbar}{k_{\rm B}T}\right)\frac{\partial\omega}{\partial V}\right\rangle_{\rm BZ} \\ &= \frac{\partial U_0}{\partial V} + \frac{\hbar}{2}\left\langle \sum \frac{\partial\omega}{\partial V}\coth\left(\frac{\hbar\omega}{2k_{\rm B}T}\right)\right\rangle_{\rm BZ} \ . \end{aligned} \tag{7}$$

From Eq. 7, we calculate the additional derivatives needed in Eq. 4

$$\frac{\partial^2 F}{\partial T \partial V} = \frac{\partial^2 U_0}{\partial T \partial V} + \frac{\hbar}{2}\left\langle \sum \left[\frac{\partial^2\omega}{\partial T\partial V}\coth\left(\frac{\hbar\omega}{2k_{\rm B}T}\right) - \frac{\partial\omega}{\partial V}\,\mathrm{csch}^2\left(\frac{\hbar\omega}{2k_{\rm B}T}\right)\left(\frac{\hbar}{2k_{\rm B}T}\frac{\partial\omega}{\partial T} - \frac{\hbar\omega}{2k_{\rm B}T^2}\right)\right]\right\rangle_{\rm BZ} \ , \tag{8}$$

and

$$\frac{\partial^2 F}{\partial V^2} = \frac{\partial^2 U_0}{\partial V^2} + \frac{\hbar}{2}\left\langle \sum \left[\frac{\partial^2\omega}{\partial V^2}\coth\left(\frac{\hbar\omega}{2k_{\rm B}T}\right) - \frac{\partial\omega}{\partial V}\,\mathrm{csch}^2\left(\frac{\hbar\omega}{2k_{\rm B}T}\right)\left(\frac{\hbar}{2k_{\rm B}T}\frac{\partial\omega}{\partial V}\right)\right]\right\rangle_{\rm BZ} \ . \tag{9}$$

C. Internal Energy

The first terms with U_0 in Eqs. 8 and 9 are familiar from the elastic energy of a solid. They are typically obtained from a Taylor expansion of the internal energy. For cubic crystals near the ground-state equilibrium volume V_0,

$$U_0(V,T) = U_0(V_0,T) + \frac{B_0(T)V_0}{2}\left(\frac{V - V_0}{V_0}\right)^2 + ... \ , \tag{10}$$

gives

$$\frac{\partial U_0}{\partial V} = B_0(T)\left(\frac{V - V_0}{V_0}\right) \ , \tag{11}$$

then

$$\frac{\partial^2 U_0}{\partial V^2} = \frac{B_0(T)}{V_0} \ , \tag{12}$$

and

$$\frac{\partial^2 U_0}{\partial T \partial V} = \frac{dB_0}{dT}\left(\frac{V - V_0}{V_0}\right) , \tag{13}$$

where $B_0 = -V(\partial P/\partial V)_{P=0}$ is the zeroth-order bulk modulus (i.e. $B_0 = B_T$).

D. Phonon Contributions at Medium to High Temperatures

To simplify the second terms in Eqs. 8 and 9, notice that $\coth(x) = \frac{1}{x} + \frac{x}{3} - \frac{x^3}{45} + \ldots$ and $\mathrm{csch}(x) = \frac{1}{x} - \frac{x}{6} + \frac{7x^3}{360} + \ldots$, so for $\hbar\omega_{\max} < k_{\mathrm{B}}T$,

$$\coth\left(\frac{\hbar\omega}{2k_{\mathrm{B}}T}\right) \simeq \mathrm{csch}\left(\frac{\hbar\omega}{2k_{\mathrm{B}}T}\right) \simeq \frac{2k_{\mathrm{B}}T}{\hbar\omega} . \tag{14}$$

Using Eq. 14 greatly simplifies Eq. 8 and 9, with the restriction to higher temperatures where $\hbar\omega_{\max} < k_{\mathrm{B}}T$,

$$\frac{\partial^2 F}{\partial T \partial V} = \frac{dB_T}{dT}\left(\frac{V - V_0}{V_0}\right) + k_{\mathrm{B}}\left\langle \sum \left(\frac{T}{\omega}\frac{\partial^2 \omega}{\partial T \partial V} - \frac{T}{\omega^2}\frac{\partial \omega}{\partial T}\frac{\partial \omega}{\partial V} + \frac{1}{\omega}\frac{\partial \omega}{\partial V}\right)\right\rangle_{\mathrm{BZ}} , \tag{15}$$

and

$$B_T = V\frac{\partial^2 F}{\partial V^2} \simeq V\left\{ \frac{B_T}{V_0} + k_{\mathrm{B}}T\left\langle \sum \left[\frac{1}{\omega}\frac{\partial^2 \omega}{\partial V^2} - \frac{1}{\omega^2}\left(\frac{\partial \omega}{\partial V}\right)^2\right]\right\rangle_{\mathrm{BZ}}\right\}$$

$$B_T = \frac{V}{V_0}B_T + k_{\mathrm{B}}TV\left\langle \sum \frac{\partial^2(\ln\omega)}{\partial V^2}\right\rangle_{\mathrm{BZ}} , \tag{16}$$

which indicates $\left| k_{\mathrm{B}}TV\left\langle \sum \frac{\partial^2(\ln\omega)}{\partial V^2}\right\rangle_{\mathrm{BZ}}\right| \ll B_T$, since $V/V_0 \simeq 1$.

E. Quasiharmonic Approximation

In the quasiharmonic approximation, $U_0 = U_0(V, T = 0)$ and $\omega = \omega(V, T = 0)$, so

$$\left(\frac{\partial^2 U_0}{\partial V^2}\right)^{\mathrm{QH}} = \frac{B_T(T=0)}{V_0} , \quad \left(\frac{\partial^2 U_0}{\partial T \partial V}\right)^{\mathrm{QH}} = 0 , \quad \left(\frac{\partial \omega}{\partial T}\right)^{\mathrm{QH}} = 0 . \tag{17}$$

For $\hbar\omega_{\max} < k_{\mathrm{B}}T$, Eqs. 8 and 9 are simplified

$$\left(\frac{\partial^2 F}{\partial T \partial V}\right)^{\mathrm{QH}} = k_{\mathrm{B}}\left\langle \sum \frac{1}{\omega(V, T=0)}\frac{\partial \omega(V, T=0)}{\partial V}\right\rangle_{\mathrm{BZ}} , \tag{18}$$

and

$$B_T^{\mathrm{QH}} = V\left(\frac{\partial^2 F}{\partial V^2}\right)^{\mathrm{QH}} \simeq \frac{V}{V_0}B_T(T=0) + k_{\mathrm{B}}TV\left\langle \sum \frac{\partial^2\left[\ln\omega(V, T=0)\right]}{\partial V^2}\right\rangle_{\mathrm{BZ}} \simeq B_T(T=0) \simeq B_T , \tag{19}$$

assuming B_T is not strongly dependent on temperature, which is often true in practice.

F. Comparison of Quasiharmonic and Anharmonic Results for Thermal Expansion

The results from Sections I D and I E allow a direct comparison of the difference in thermal expansion predicted by anharmonic and quasiharmonic theory. For moderate to high temperatures the difference between β and β^{QH} is

$$\beta - \beta^{\mathrm{QH}} = \left(-\frac{1}{B_T}\frac{\partial^2 F}{\partial T \partial V}\right) - \left(-\frac{1}{B_T^{\mathrm{QH}}}\frac{\partial^2 F^{\mathrm{QH}}}{\partial T \partial V}\right) ,$$

$$\simeq -\frac{1}{B_T}\frac{\partial^2\left(F - F^{\mathrm{QH}}\right)}{\partial T \partial V} ,$$

assuming the bulk modulus does not vary strongly with temperature. Using the derivatives of F from Sections I D and I E

$$\begin{aligned}
\beta - \beta^{\mathrm{QH}} &= -\frac{1}{B_T}\frac{dB_T}{dT}\left(\frac{V-V_0}{V_0}\right) - \\
&\quad \frac{k_{\mathrm{B}}}{B_T}\left\langle \sum \left(\frac{T}{\omega}\frac{\partial^2\omega}{\partial T \partial V} - \frac{T}{\omega^2}\frac{\partial \omega}{\partial T}\frac{\partial \omega}{\partial V} + \frac{1}{\omega(V,T)}\frac{\partial \omega(V,T)}{\partial V} - \frac{1}{\omega(V,T=0)}\frac{\partial \omega(V,T=0)}{\partial V} \right) \right\rangle_{\mathrm{BZ}} \\
&\simeq -\frac{1}{B_T}\frac{dB_T}{dT}\left(\frac{V-V_0}{V_0}\right) - \frac{k_{\mathrm{B}}}{B_T}\left\langle \sum \left[\frac{T}{\omega}\frac{\partial^2\omega}{\partial T \partial V} - \frac{T}{\omega^2}\frac{\partial \omega}{\partial T}\frac{\partial \omega}{\partial V} + T\frac{\partial}{\partial T}\left(\frac{1}{\omega}\frac{\partial \omega}{\partial V}\right) \right] \right\rangle_{\mathrm{BZ}} \\
&= -\frac{1}{B_T}\frac{dB_T}{dT}\left(\frac{V-V_0}{V_0}\right) - \frac{2k_{\mathrm{B}}}{B_T}\left\langle \sum \left(\frac{T}{\omega}\frac{\partial^2\omega}{\partial T \partial V} - \frac{T}{\omega^2}\frac{\partial \omega}{\partial T}\frac{\partial \omega}{\partial V} \right) \right\rangle_{\mathrm{BZ}} \\
&= -\frac{1}{B_T}\frac{dB_T}{dT}\left(\frac{V-V_0}{V_0}\right) + \frac{2k_{\mathrm{B}}T}{B_T}\left\langle \sum \left(-\frac{1}{\omega}\frac{\partial^2\omega}{\partial T \partial V} + \frac{1}{\omega^2}\frac{\partial \omega}{\partial T}\frac{\partial \omega}{\partial V} \right) \right\rangle_{\mathrm{BZ}} ,
\end{aligned} \tag{20}$$

thus we have

$$\begin{aligned}
\beta^{\mathrm{QH}} \Big/ \beta &= 1 + \frac{1}{B_T\beta}\frac{dB_T}{dT}\left(\frac{V-V_0}{V_0}\right) - \frac{2k_{\mathrm{B}}T}{B_T\beta}\left\langle \sum \left(-\frac{1}{\omega}\frac{\partial^2\omega}{\partial T \partial V} + \frac{1}{\omega^2}\frac{\partial \omega}{\partial T}\frac{\partial \omega}{\partial V} \right) \right\rangle_{\mathrm{BZ}} \\
&\simeq 1 - \frac{2k_{\mathrm{B}}T}{B_T\beta}\left\langle \sum \left(-\frac{1}{\omega}\frac{\partial^2\omega}{\partial T \partial V} + \frac{1}{\omega^2}\frac{\partial \omega}{\partial T}\frac{\partial \omega}{\partial V} \right) \right\rangle_{\mathrm{BZ}} ,
\end{aligned} \tag{21}$$

since $\frac{1}{B_T\beta}\frac{dB_T}{dT}\left(\frac{V-V_0}{V_0}\right) < \frac{1}{B_T\beta}\frac{dB_T}{dT}\beta T = \left(\frac{dB_T}{dT}T\right)\Big/ B_T \sim 0.1 \ll 1$ (e.g. in MgO [5]).

G. Simplifying Parameters

Introducing the mode Grüneisen parameter,

$$\gamma_v \triangleq -\frac{V}{\omega}\left(\frac{\partial \omega}{\partial V}\right)\Big|_T , \tag{22}$$

the thermal Grüneisen parameter (unitless),

$$\gamma_T \triangleq -\frac{T}{\omega}\left(\frac{\partial \omega}{\partial T}\right)\Big|_V , \tag{23}$$

and the anharmonicity parameter (unitless),

$$\gamma_{V,T} \triangleq -\frac{VT}{\omega}\left(\frac{\partial^2 \omega}{\partial T \partial V}\right) , \tag{24}$$

Eq. 21 can be rewritten as

$$\beta^{\mathrm{QH}} \Big/ \beta = 1 - \frac{2k_{\mathrm{B}}}{B_T\beta V}\left\langle \sum \left(\gamma_{V,T} + \gamma_T\gamma_V\right) \right\rangle_{\mathrm{BZ}} . \tag{25}$$

Normally, we have $\gamma_T \sim \mathcal{O}(10^{-1})$ [1] and $\gamma_V \sim \mathcal{O}(10^{0\sim1})$. Thus, in highly anharmonic solids with $\gamma_{V,T} \sim \mathcal{O}(1)$, the anharmonicity parameter becomes the dominant term, which gives

$$\beta^{\mathrm{QH}} \Big/ \beta \simeq 1 - \frac{2k_{\mathrm{B}}}{B_T\beta V}\left\langle \sum \gamma_{V,T} \right\rangle_{\mathrm{BZ}} = 1 - \frac{2k_{\mathrm{B}}}{B_T\beta V}(3N)\overline{\gamma}_{V,T} = 1 - \frac{6k_{\mathrm{B}}}{B_T\beta v}\overline{\gamma}_{V,T} , \tag{26}$$

where $v = V/N$ is the volume per atom, and $\overline{\gamma}_{V,T} = \frac{1}{3N}\left\langle \sum_{\mathbf{k}}\sum_{j=1}^{3N}\gamma_{V,T}^{(j)} \right\rangle_{\mathrm{BZ}}$ is the average anharmonicity parameter.

An interesting and compact result from Eq. 26 is

$$\beta \simeq \beta^{\mathrm{QH}} + \frac{6k_{\mathrm{B}}}{B_T v}\overline{\gamma}_{V,T} . \tag{27}$$

This shows that the thermal expansion differs from that of the QHA owing to the mixed second derivative of the phonon energy of Eq. 24. In general, thermal expansion requires the consideration of both the volume and temperature dependence of the free energy.

H. Why is the QHA Unreliable for Thermal Expansion?

Eq. 27 shows why the quasiharmonic model predicts a small thermal expansion coefficient when phonon frequencies have a temperature dependence that varies with volume. Only in the limit of no temperature dependence, which means $\overline{\gamma}_{V,T} = 0$, Eq. 27 reduces to $\beta^{\rm QH} = \beta$. Here we estimate some magnitudes of these effects.

The change of internal energy is estimated as

$$\Delta U_0 = \frac{1}{2} B_0 V_0 \left(\frac{\Delta V}{V_0}\right)^2 \simeq B_0 V \cdot (0.01)^2 \simeq 10^{0\sim1}\text{meV} \,, \tag{28}$$

which gives

$$B_T V = B_0 V \simeq 10^{4\sim5}\,\text{meV} = 10^{1\sim2}\,\text{eV} \,. \tag{29}$$

Thus,

$$\frac{6k_{\rm B}}{B_T \beta V} \simeq \frac{6 \times 8.617 \times 10^{-5}\,\text{eV}\cdot\text{K}^{-1}}{10^{-5\sim-4}\,\text{K}^{-1}\cdot 10^{1\sim2}\,\text{eV}} \sim \mathcal{O}\left(10^{-2\sim0}\right) \text{ [unitless]} \,, \tag{30}$$

and in some solids, some modes are possible with $0 < \overline{\gamma}_{V,T} \sim \mathcal{O}(1)$.

Finally, we have

$$\beta^{\rm QH} \Big/ \beta \sim 1 - \mathcal{O}\left(10^{-2\sim0}\right) \cdot \mathcal{O}(1) \,. \tag{31}$$

Under some circumstances, the thermal expansion coefficient can be several times larger than the quasiharmonic prediction, which means the QHA fails to get the first-order term for thermal expansion. If the QHA accounts for the leading term of thermal expansion, it is either because 1) the solid is not so anharmonic ($\overline{\gamma}_{V,T}$ is small), or 2) there is a cancellation of positive and negative $\overline{\gamma}_{V,T}$ for different phonon modes despite the anharmonicity.

I. Estimate of Thermal Expansion of NaBr

To obtain these $\gamma_{V,T}$, we need the phonon frequencies on a temperature-volume (T-V) grid to calculate the second derivative of $\dfrac{\partial^2\omega(T,V)}{\partial T \partial V}$. It is risky to perform such approximation with limited experimental data (phonon information at only three T-V points). We developed an alternative way to obtain this mixed derivative using our richer set of computational results that provided the phonon DOS on a 5×5 T-V grid for predicting the thermal expansion. (These calculated anharmonic phonons proved reliable by comparing with the experimental results at the equilibrium volumes at 10, 300 and 700 K.)

For $\omega(T,V)$, the Taylor expansion to second order gives

$$\begin{aligned} \Delta\omega &= \omega(T+\Delta T, V+\Delta V) - \omega(T,V) \,, & (32)\\ &\simeq \frac{\partial\omega}{\partial T}\Delta T + \frac{\partial\omega}{\partial V}\Delta V \\ &\quad + \frac{1}{2}\left(\frac{\partial^2\omega}{\partial T^2}(\Delta T)^2 + 2\frac{\partial^2\omega}{\partial T\partial V}(\Delta T \Delta V) + \frac{\partial^2\omega}{\partial V^2}(\Delta V)^2\right) \,. & (33) \end{aligned}$$

The first two terms in Eq. 33, with linear shifts of frequency with ΔT and ΔV, give the shifts from anharmonicity and quasiharmonicity. The term in $(\Delta T)^2$ is beyond the anharmonicity from cubic and quartic perturbations, which give frequency shifts linear in ΔT. We expect it to be smaller in the anharmonic effects of NaBr at constant volume (the alternative would be exotic).

The remaining term in Eq. 33 with $\Delta T \Delta V$ describes how a Grüneisen parameter changes with temperature, or how the anharmonicity changes with volume. If mode Grüneisen parameters change with temperature, the anharmonic 3- and 4-phonon processes will have a different dependence on volume at low and high temperatures, owing to changes in the kinematically-allowed 3- and 4-phonon processes that conserve energy and momentum. This is a change in anharmonicity with volume.

$$\Delta\omega \simeq \frac{\partial\omega}{\partial T}\Delta T + \frac{\partial\omega}{\partial V}\Delta V + \frac{\partial^2\omega}{\partial T\partial V}(\Delta T\Delta V) + \frac{1}{2}\frac{\partial^2\omega}{\partial V^2}(\Delta V)^2 \,. \tag{34}$$

The second term in Eq. 34, the quasiharmonic correction, is a first order term. It is expected to be larger than the third term. However, the temperature dependence is still needed for thermal expansion, so the third term proves important.

Therefore, we fit the phonon frequencies with

$$\omega(T,V) = \omega_0 + a*T + b*(V-V_0) + c*T*(V-V_0) + d*(V-V_0)^2\,, \tag{35}$$

where ω and ω_0 are in units of meV, T is in K, and V and V_0 are in Å^3. (The constant V_0, which emphasizes the role of volume changes, was set as the smallest volume on the T-V grid evaluated during the fitting process.) By the least-square method, we got the following fitting parameters (units ignored):

$$\omega(T,V) = 13.50 - 9.731\times10^{-4}T - 0.924(V-27) - 2.869\times10^{-4}\cdot T(V-27) + 2.554\times10^{-2}(V-27)^2 \tag{36}$$

The coefficient of determination is $R^2 = 0.9668$, indicating Eq. 35 is a suitable choice. The derived unitless parameters are $\overline{\gamma}_T \simeq 0.1$, $\overline{\gamma}_V \simeq 1.6$, $\overline{\gamma}_{V,T} \simeq 0.6$. The relative contributions to the averaged anharmonicity parameter, $\overline{\gamma}_{V,T}$, from individual phonon modes are shown in Fig. 1.

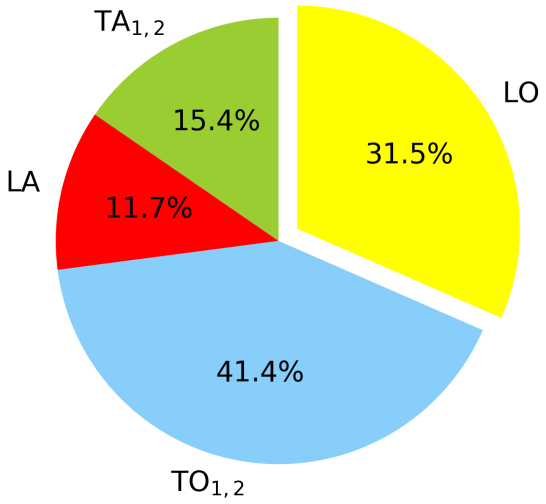

FIG. 1. **The relative contributions to the averaged anharmonicity parameter.** It shows that the optical phonons (especially LO) contribute most to the anharmonicity parameter.

We take the value of $\beta = 3\alpha = 3\times60.63\times10^{-6}\,\text{K}^{-1} = 182\times10^{-6}\,\text{K}^{-1}$ [6], $B_T = 18.5\,\text{GPa}$ [7] and $a = 6.1376\,\text{Å}\,(700\,\text{K})$ [6], which gives the volume per atom as $v = a^3/8 = 2.89\times10^{-29}\,\text{m}^3$. So finally, due to the dominance of $\overline{\gamma}_{V,T}$, we can roughly estimate that

$$\beta^{\text{QH}}\Big/\beta = 1 - \frac{6k_\text{B}}{B_T\beta v}\overline{\gamma}_{V,T} \simeq 0.48\,. \tag{37}$$

Or by using a more rigorous relation, we have

$$\beta^{\text{QH}}\Big/\beta = 1 - \frac{6k_\text{B}}{B_T\beta v}\left(\overline{\gamma}_{V,T} + \overline{\gamma}_V\overline{\gamma}_T\right) \simeq 0.35\,. \tag{38}$$

II. INELASTIC NEUTRON SCATTERING EXPERIMENTS

A. Details about the experiment

The INS measurements used a high-purity single crystal of NaBr. Crystal quality was checked by X-ray and neutron diffraction. The INS data were acquired with the time-of-flight Wide Angular-Range Chopper Spectrometer, ARCS,

at the Spallation Neutron Source at the Oak Ridge National Laboratory. The neutrons had an incident energy of 30 meV. The single crystal of [001] orientation was suspended in an aluminum holder, which was mounted in a closed-cycle helium refrigerator for the 10 K measurement, and a low-background electrical resistance vacuum furnace for measurements at 300 and 700 K. For each measurement, time-of-flight neutron data was collected from 201 rotations of the crystal in increments of 0.5° about the vertical axis.

Data reduction gave the 4D scattering function $S(\mathbf{Q},\varepsilon)$, where $\mathbf{Q}$ is the 3D wave-vector and ε is the phonon energy (from the neutron energy loss). Measurements with an empty can were performed to evaluate the background. To correct for nonlinearities of the ARCS instrument, offsets of the q-grid were corrected to first order by fitting a set of 45 *in situ* Bragg diffractions, which were transformed to their theoretical positions in the reciprocal space of the NaBr structure. The linear transformation matrix had only a small deviation (less than 0.02) from the identity matrix, showing that the original data had good quality and the linear correction for q-offsets was adequate. After subtracting the empty-can background and removing multiphonon scattering calculated with the incoherent approximation (discussed below), the intensities from the higher Brillouin zones were folded back into an irreducible wedge in the first Brillouin zone to obtain the spectral intensities shown in Fig. 2 in the main text.

The multiphonon scattering in the incoherent approximation [8] is given by

$$S_{n>1}(\mathbf{Q},\varepsilon) = \sum_{n=2}^{\infty}\sum_{d} e^{-2W_d}\frac{(2W_d)^n}{n!}\frac{\sigma_{\text{total},d}}{M_d}A_{n,d}(\varepsilon)\ , \tag{39}$$

where $\mathbf{Q}$ is the reciprocal space vector, ε is the phonon energy, and for atom $d \in (\text{Na},\text{Br})$, $\sigma_{\text{total},d}$ is the total neutron scattering cross section, M_d is atomic mass, and

$$2W_d = 2W_d(|\mathbf{Q}|) = \frac{\hbar^2|\mathbf{Q}|^2}{2M_d}\int_0^{\infty} d\varepsilon\ \frac{g_d(\varepsilon)}{\varepsilon}\coth\left(\frac{\varepsilon}{2k_BT}\right) \tag{40}$$

is the Debye-Waller factor. The n^{th}-order partial phonon spectra of atoms d and $\bar{d}$, $A_{n,d}$ and $A_{n,\bar{d}}$, were calculated as

$$A_{1,d}(\varepsilon) = \frac{g_d(\varepsilon)}{\varepsilon}\frac{1}{e^{\varepsilon/k_BT}-1}\ , \tag{41}$$

$$A_{1,\bar{d}}(\varepsilon) = \frac{g_{\bar{d}}(\varepsilon)}{\varepsilon}\frac{1}{e^{\varepsilon/k_BT}-1}\ , \tag{42}$$

$$A_{n,d}(\varepsilon) = \frac{1}{2}\left(A_{1,d}\circledast A_{n-1,d} + \frac{1}{n}A_{1,d}\circledast A_{n-1,\bar{d}} + \frac{n-1}{n}A_{1,\bar{d}}\circledast A_{n-1,d}\right)\ , \tag{43}$$

$$A_{n,\bar{d}}(\varepsilon) = \frac{1}{2}\left(A_{1,\bar{d}}\circledast A_{n-1,\bar{d}} + \frac{1}{n}A_{1,\bar{d}}\circledast A_{n-1,d} + \frac{n-1}{n}A_{1,d}\circledast A_{n-1,\bar{d}}\right)\ . \tag{44}$$

Here, $\bar{d}$ refers to the other atom in the unit cell. The temperature-dependent partial phonon density of states (DOS), $g_d(\varepsilon)$, was obtained by our sTDEP method that used *ab initio* DFT calculations.

For NaBr, we truncated Eq. 39 at $n = 8$, and a global scaling factor was applied to the multiphonon scattering function for normalization. Finally, the folded-back data was corrected for the phonon creation thermal factor. This folding technique cancels out the polarization effects and improves the statistical quality by assessing phonon intensities over multiple Brillouin zones. Fig. 2 shows a set of enlarged, separated figures of the scattering data along the Γ-X and Γ-L directions.

B. Extracting the phonon DOS

Since the thermal expansion is now obtained from a free energy in which the phonon contribution was determined by the phonon DOS, we also confirmed that the anharmonic phonon DOS at elevated temperatures agrees with the experimentally-measured phonon DOS. This is shown in Fig. 3. Because the measurements were on a single crystal, the phonon DOS was obtained by integration of the first Brillouin zone after folding back the inelastic neutron scattering data from higher zones. This method is not so well established as simpler measurements on powder samples. Fortunately the effects from alignment of scattering vectors along the polarization vectors of phonons should be largely absent when more Brillouin zones were folded back. There are also effects from instrument resolution function and multiple scattering in a large crystal. These effects could distort the intensities of the different peaks in the phonon DOS, but the energies of the peaks should be reliable. These results are good enough to establish the reliability of our anharmonic phonon calculations at elevated temperatures.

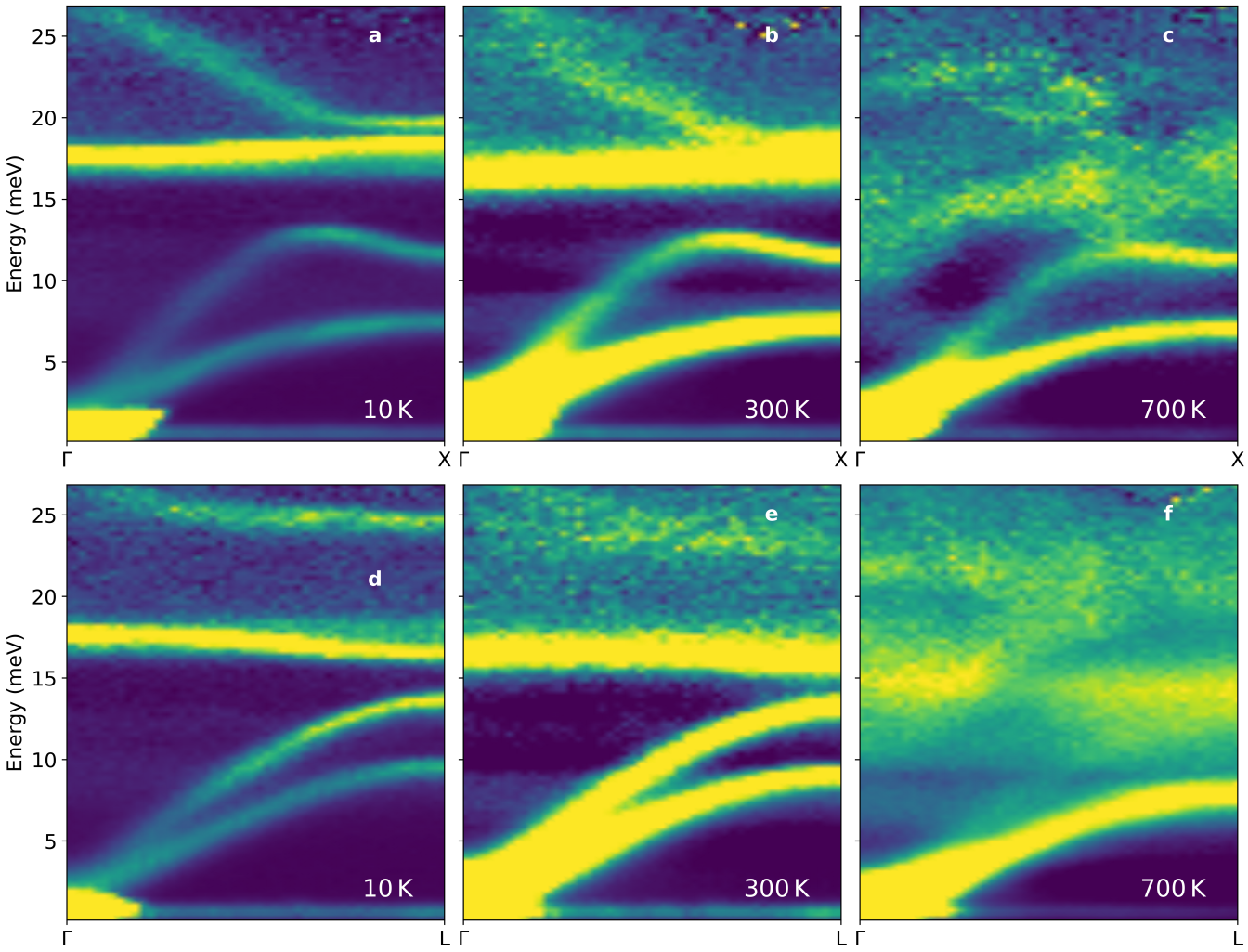

FIG. 2. **Experimental phonon dispersions of NaBr along Γ-X and Γ-L.** Phonon dispersions are shown by 2D slices of the $S(\mathbf{Q}, \varepsilon)$ data along the high symmetry lines of Γ-X **(a-c)** and Γ-L **(d-f)** at the temperature of 10 K **(a, d)**, 300 K **(b, e)** and 700 K **(c, f)**.

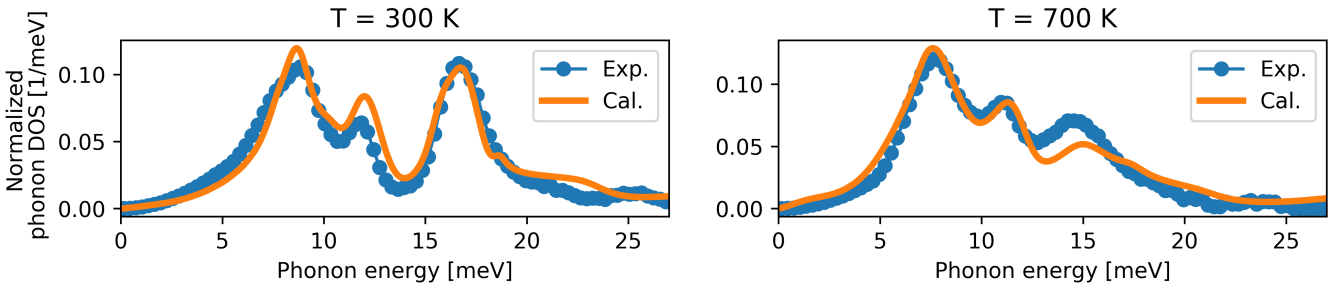

FIG. 3. **Comparison between the experimental phonon DOS extracted from the INS data and the calculated anharmonic phonon DOS at elevated temperatures: 300 K (left) and 700 K (right).**

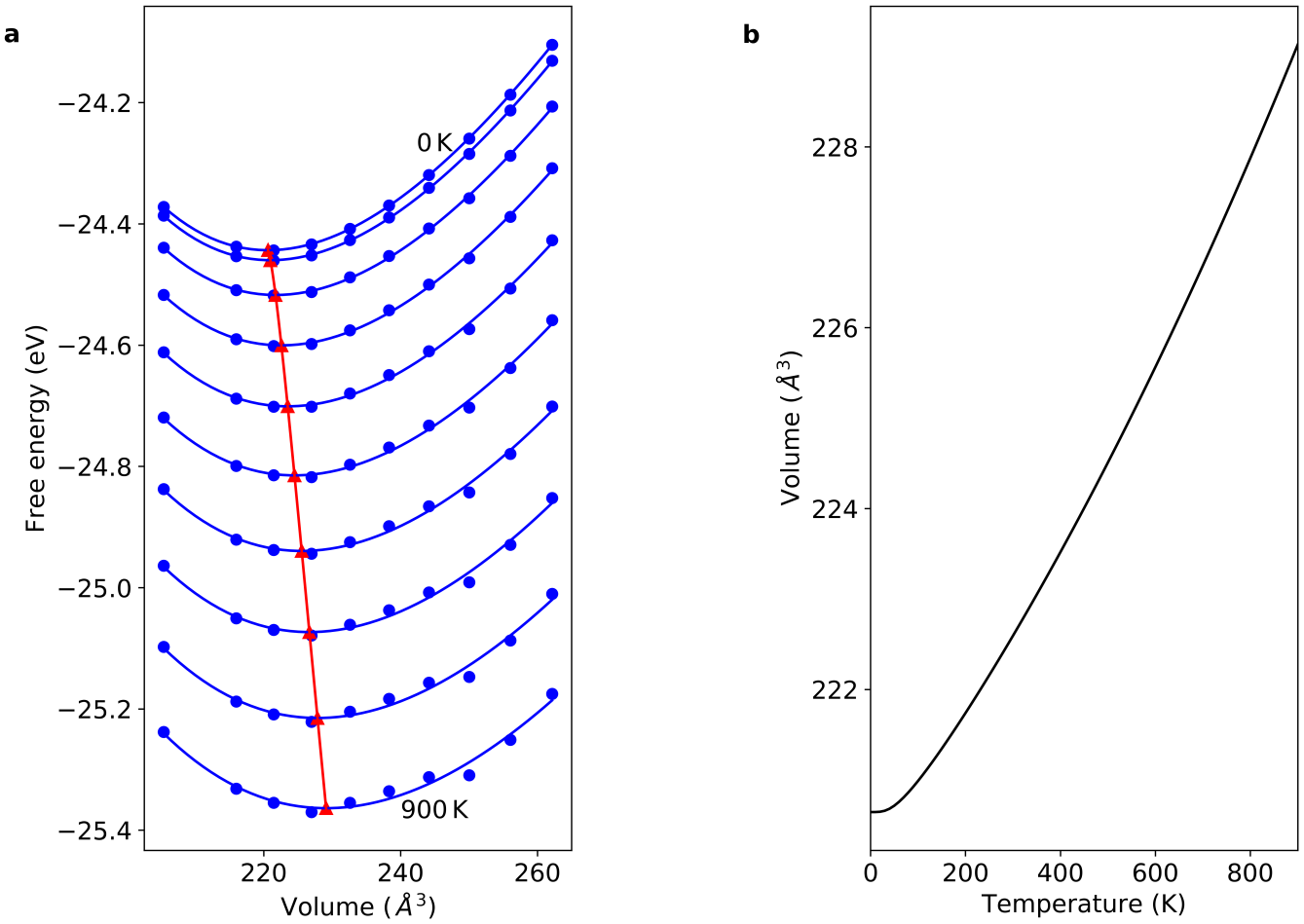

FIG. 4. **Intermediate results for expansion coefficients of NaBr calculated with the QHA. a,** The Helmholtz free energy as a function of temperature and volume. The volume-energy data was fitted to a Birch-Murnaghan equation of state. **b,** The equilibrium volumes with temperature, obtained by minimizing the free energy at each temperature.

III. AB INITIO CALCULATIONS

A. General

All DFT calculations were performed with the VASP package using a plane-wave basis set [9–12] with projector augmented wave (PAW) pseudopotentials [13] and the Perdew-Burke-Ernzerhof (PBE) exchange correlation functional [14]. All calculations used a kinetic-energy cutoff of 550 meV, a 5×5×5 supercell of 250 atoms, and a 3×3×3 k-point grid. Quasiharmonic calculations used PHONOPY [15]. The sTDEP [16–18] method was used to calculate anharmonic phonons at elevated temperatures. The Born effective charges and dielectric constants were obtained by DFT calculations in VASP [19]. The non-analytical term of the long-ranged electrostatics was corrected for both quasiharmonic and anharmonic calculations [20]. The phonon self-energy was calculated with a 35×35×35 q-grid.

B. Quasiharmonic calculations

The free energy and the equilibrium volumes calculated with the QHA are shown in Fig. 4. The linear thermal expansion coefficients from measurements and QHA calculations are compared in Fig. 5. We did not calculate detailed linear thermal expansion coefficients with the stochastically-initialized temperature dependent effective potential method (sTDEP) method, but we compared lattice constants at several temperatures to illustrate thermal expansion (see Fig. 1 in the main text).

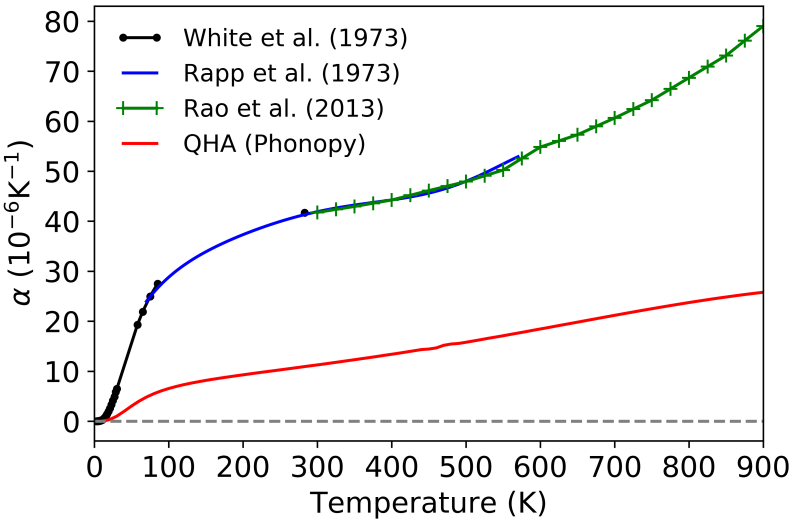

FIG. 5. **Thermal expansion coefficients of NaBr, measured and calculated by QHA.** The *ab initio* quasiharmonic predictions (red solid line) are compared to the experimental results [6, 21, 22]. The linear thermal expansion coefficients, α, are a factor of four lower than experimental results.

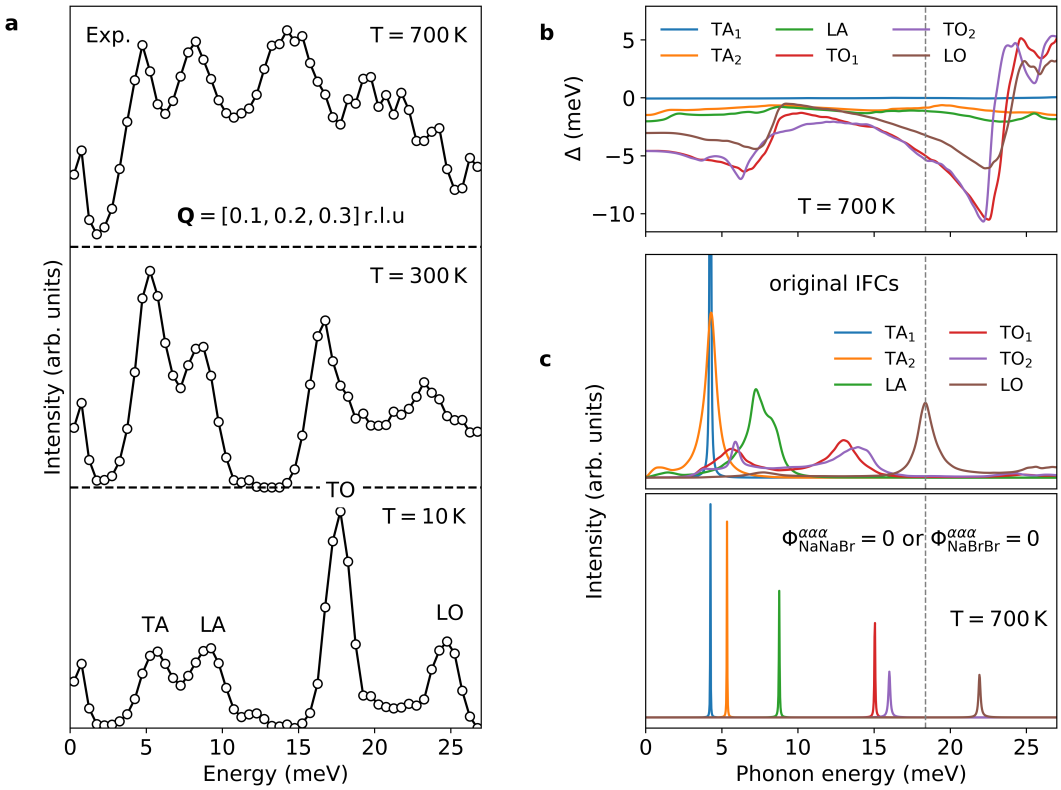

FIG. 6. **Measured and calculated phonon lineshapes at $\mathbf{Q} = [0.1, 0.2, 0.3]$ r.l.u. and the real part of the phonon self-energy. a,** The 1D cut of $S(\mathbf{Q}, \varepsilon)$ at a constant $\mathbf{Q} = [0.1, 0.2, 0.3]$ r.l.u. (reciprocal lattice units), showing the temperature dependence of phonon lineshapes in NaBr. At this Q-point, the LO phonon peak has an energy decrease with temperature of $3 \sim 4$ meV. This can be attributed to the real component of the phonon self-energy as shown in **(b)**. The intensity data were scaled and offset for clarity. **c,** By nulling the third-order force constants, $\Phi^{\alpha\alpha\alpha}_{\mathrm{NaNaBr}}$ or $\Phi^{\alpha\alpha\alpha}_{\mathrm{NaBrBr}}$, associated with the nearest-neighbor degenerate triplets, where $\alpha = (x, y, z)$ represents the direction along the Na-Br bond, the lineshapes at this Q-point become narrow Lorentzian peaks at 700 K and the energy decrease of the LO mode vanishes.

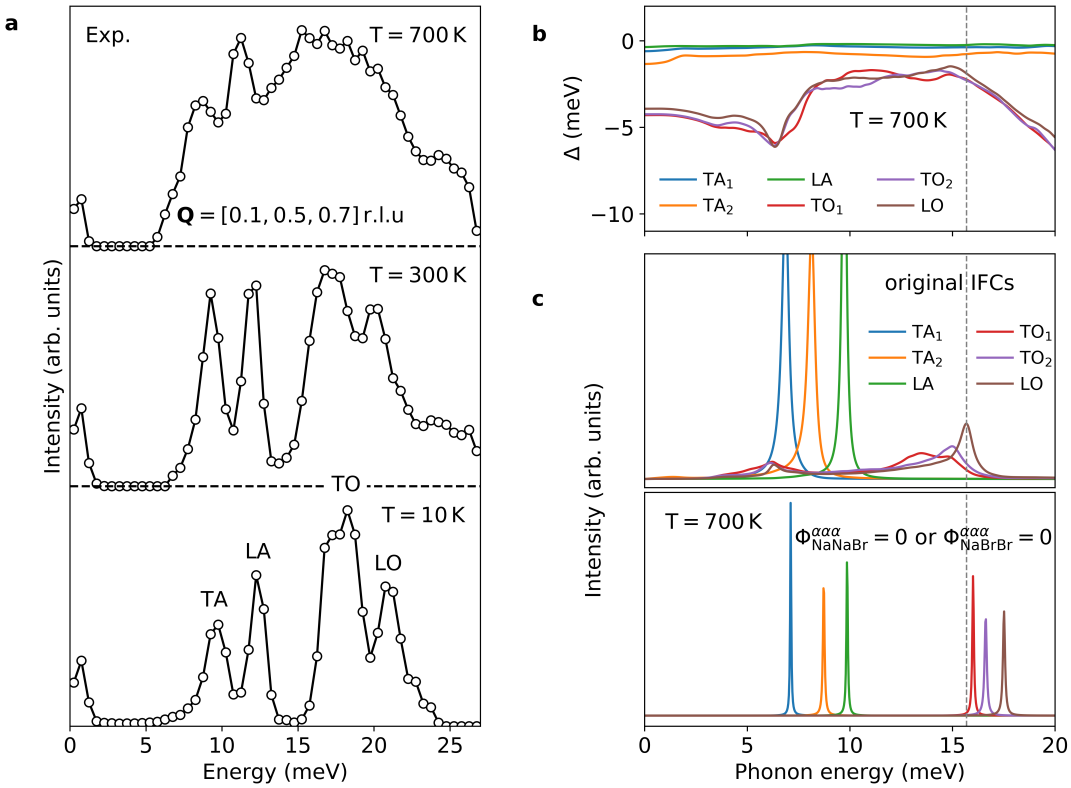

FIG. 7. **Measured and calculated phonon lineshapes at $\mathbf{Q} = [0.1, 0.5, 0.7]$ r.l.u. and the real part of the phonon self-energy.** The panels are the same quantities in the previous figure, but for $\mathbf{Q} = [0.1, 0.5, 0.7]$ r.l.u. It is seen again that the LO phonon mode shifts to a lower energy at 700 K, mainly due to the cubic interactions.

C. Anharmonic calculations: sTDEP method

With harmonic forces, the instantaneous position ($\mathbf{u_i}$) and velocity ($\dot{\mathbf{u}}_i$) of the ith atom are the sums of contributions from $3N$ normal modes

$$\mathbf{u}_i = \sum_{s=1}^{3N} \boldsymbol{\epsilon}_{is} A_{is} \sin(\omega_s t + \delta_s) \,, \tag{45}$$

$$\dot{\mathbf{u}}_i = \sum_{s=1}^{3N} \boldsymbol{\epsilon}_{is} A_{is} \omega_s \cos(\omega_s t + \delta_s) \,, \tag{46}$$

where A_s is the normal mode amplitude, δ_s is the phase shift, ω_s and $\boldsymbol{\epsilon}_s$ are eigenvalue and eigenvector corresponding to mode s.

To obtain a set of positions and velocities that correspond to a canonical ensemble, we choose the A_s and δ_s so they are normally distributed around their mean value. Each mode s should contribute, on average, $k_{\mathrm{B}}T/2$ to the internal energy. Then

$$\langle A_{is} \rangle = \sqrt{\frac{\hbar(2n_s + 1)}{2m_i\omega_s}} \approx \frac{1}{\omega_s}\sqrt{\frac{k_{\mathrm{B}}T}{m_i}} \,, \tag{47}$$

where the approximate result is in the classical limit, $\hbar\omega \ll k_{\mathrm{B}}T$. The appropriate distribution of atomic positions

and velocities are

$$\mathbf{u}_i = \sum_{s=1}^{3N} \boldsymbol{\epsilon}_{is} \langle A_{is} \rangle \sqrt{-2 \ln \xi_1} \sin 2\pi\xi_2 \ , \tag{48}$$

$$\dot{\mathbf{u}}_i = \sum_{s=1}^{3N} \omega_s \boldsymbol{\epsilon}_{is} \langle A_{is} \rangle \sqrt{-2 \ln \xi_1} \cos 2\pi\xi_2 \ , \tag{49}$$

where $\xi_n (n = 1, 2)$ represent a uniform distribution of random numbers between $(0, 1)$, which are transformed to a normal distribution using the standard Box-Muller transform [23, 24].

In practice, we performed first-principles calculations on a temperature-volume grid covering five temperatures and five volumes. We chose the five temperatures as $T = \{10, 300, 450, 600, 700\}$ K and the five volumes linearly spaced within $\pm 5\%$ around the equilibrium volumes. We iterated for 3 to 5 times until the force constants were converged.

Using results from many-body theory, the phonon frequencies were obtained from the dynamical matrix for the constants $\{\Phi_{ij}\}$, and then corrected by the real (Δ) and imaginary (Γ) parts of the phonon self-energy. The imaginary part of the phonon self-energy was calculated with the third-order force constants,

$$\begin{aligned} \Gamma_\lambda(\Omega) = \frac{\hbar\pi}{16} \sum_{\lambda'\lambda''} |\Phi_{\lambda\lambda'\lambda''}|^2 \big\{ & (n_{\lambda'} + n_{\lambda''} + 1) \\ & \times \delta(\Omega - \omega_{\lambda'} - \omega_{\lambda''}) + (n_{\lambda'} - n_{\lambda''}) \\ & \times [\delta(\Omega - \omega_{\lambda'} + \omega_{\lambda''}) - \delta(\Omega + \omega_{\lambda'} - \omega_{\lambda''})] \big\} \ , \end{aligned} \tag{50}$$

where $\Omega (= E/\hbar)$ is the probing energy. The real part was obtained by a Kramers-Kronig transformation

$$\Delta(\Omega) = \mathcal{P} \int \frac{1}{\pi} \frac{\Gamma(\omega)}{\omega - \Omega} \mathrm{d}\omega \ . \tag{51}$$

Equation 50 is a sum over all possible three-phonon interactions, where $\Phi_{\lambda\lambda'\lambda''}$ is the three-phonon matrix element obtained from the cubic force constants Φ_{ijk} by Fourier transformation, n is the Bose-Einstein thermal occupation factor giving the number of phonons in each mode, and the delta functions conserve energy and momentum.

IV. PHONONS AWAY FROM HIGH SYMMETRY LINES

The anharmonicity and its origin with first-neighbor Na-Br bonds are not only true for phonons along the high-symmetry lines, but for the whole Brillouin zone. Figures 6 and 7 (similar to Fig. 3 in the manuscript) show lineshapes from experiment and computation at two arbitrary points in the Brillouin zone, along with the calculated real part of the phonon self-energy. The thermal softening of the LO phonon modes at 700 K is seen over the Brillouin zone. The real part of the phonon self-energy, arising from cubic anharmonicity to second order, is the main cause of these thermal shifts and broadenings.

[1] P. B. Allen, Quasi-harmonic theory of thermal expansion, arXiv preprint arXiv:1906.07103 (2019).
[2] D. C. Wallace, *Statistical Physics of Crystals and Liquids* (World Scientific, Singapore, 2002) p. 193.
[3] R. A. Cowley, Zero sound, first sound and second sound of solids, Proc. Phys. Soc. **90**, 1127 (1967).
[4] J. A. Reissland, *The Physics of Phonons* (Wiley-Interscience, London, UK, 1973) Chap. 7.4.
[5] O. L. Anderson, Derivation of Wachtman's equation for the temperature dependence of elastic moduli of oxide compounds, Phys. Rev. **144**, 553 (1966).
[6] A. S. M. Rao, K. Narender, K. G. K. Rao, and N. G. Krishna, Thermophysical properties of NaCl, NaBr and NaF by γ-ray attenuation technique, J. Mod. Phys. **4**, 208 (2013).
[7] Y. Sato-Sorensen, Phase transitions and equations of state for the sodium halides: NaF, NaCl, NaBr, and NaI, J. Geophys. Res. Solid Earth **88**, 3543 (1983).
[8] V. F. Sears, Incoherent neutron scattering for large momentum transfer. ii. quantum effects and applications, Phys. Rev. A **7**, 340 (1973).
[9] G. Kresse and J. Hafner, *Ab initio* molecular dynamics for liquid metals, Phys. Rev. B **47**, 558 (1993).
[10] G. Kresse and J. Hafner, *Ab initio* molecular-dynamics simulation of the liquid-metal–amorphous-semiconductor transition in germanium, Phys. Rev. B **49**, 14251 (1994).

[11] G. Kresse and J. Furthmüller, Efficiency of ab-initio total energy calculations for metals and semiconductors using a plane-wave basis set, Comput. Mater. Sci. **6**, 15 (1996).
[12] G. Kresse and J. Furthmüller, Efficient iterative schemes for *ab initio* total-energy calculations using a plane-wave basis set, Phys. Rev. B **54**, 11169 (1996).
[13] G. Kresse and D. Joubert, From ultrasoft pseudopotentials to the projector augmented-wave method, Phys. Rev. B **59**, 1758 (1999).
[14] J. P. Perdew, K. Burke, and M. Ernzerhof, Generalized gradient approximation made simple, Phys. Rev. Lett. **77**, 3865 (1996).
[15] A. Togo and I. Tanaka, First principles phonon calculations in materials science, Scr. Mater. **108**, 1 (2015).
[16] O. Hellman, I. A. Abrikosov, and S. I. Simak, Lattice dynamics of anharmonic solids from first principles, Phys. Rev. B **84**, 180301 (2011).
[17] O. Hellman, P. Steneteg, I. A. Abrikosov, and S. I. Simak, Temperature dependent effective potential method for accurate free energy calculations of solids, Phys. Rev. B **87**, 104111 (2013).
[18] O. Hellmanand I. A. Abrikosov, Temperature-dependent effective third-order interatomic force constants from first principles, Phys. Rev. B **88**, 144301 (2013).
[19] M. Gajdoš, K. Hummer, G. Kresse, J. Furthmüller, and F. Bechstedt, Linear optical properties in the projector-augmented wave methodology, Phys. Rev. B **73**, 045112 (2006).
[20] X. Gonze and C. Lee, Dynamical matrices, born effective charges, dielectric permittivity tensors, and interatomic force constants from density-functional perturbation theory, Phys. Rev. B **55**, 10355 (1997).
[21] G. K. White, J. G. Collins, and K. A. G. Mendelssohn, The thermal expansion of alkali halides at low temperatures - II. Sodium, rubidium and caesium halides, Proc. R. Soc. Lond. A **333**, 237 (1973).
[22] J. E. Rapp and H. D. Merchant, Thermal expansion of alkali halides from 70 to 570 K, J. Appl. Phys. **44**, 3919 (1973).
[23] D. C. Wallace, *Thermodynamics of crystals* (Wiley, New York, US, 1972).
[24] N. Shulumba, O. Hellman, and A. J. Minnich, Intrinsic localized mode and low thermal conductivity of PbSe, Phys. Rev. B **95**, 014302 (2017).